

Tevatron Potential for Technicolor Search with Prompt Photons.

Alexander Belyaev^{1,2}, Rogerio Rosenfeld¹ and Alfonso R. Zerwekh¹

¹ *Instituto de Física Teórica, Universidade Estadual Paulista,*

Rua Pamplona 145, 01405-900 - São Paulo, S.P., Brazil

² *Skobeltsyn Institute for Nuclear Physics, Moscow State University,*

119 899, Moscow, Russian Federation

Abstract

We perform a detailed study of the process of single color octet isoscalar η_T production at the Tevatron with $\eta_T \rightarrow \gamma + g$ decay signature, including a complete simulation of signal and background processes. We determined a set of optimal cuts from an analysis of the various kinematical distributions for the signal and backgrounds. As a result we show the exclusion and discovery limits on the η_T mass which could be established at the Tevatron for some technicolor models.

12.60.Nz, 12.60.Fr

I. INTRODUCTION

The Standard Model has been extensively tested and it is a very successful description of the weak interaction phenomenology. Nevertheless, the electroweak symmetry breaking sector has essentially remained unexplored. In the Standard Model, the Higgs boson plays a crucial rôle in the symmetry breaking mechanism. However, the presence of such a fundamental scalar at the 100 GeV scale gives rise to some theoretical problems, such as the naturalness of a light Higgs boson and the triviality of the fundamental Higgs self-interaction. These problems lead to the conclusion that the Higgs sector of the Standard Model is in fact a low energy effective description of some new Physics at a higher energy scale.

Three main avenues for the new Physics have been proposed: low-scale supersymmetry [1], large extra dimensions at TeV scale [2] and dynamical symmetry breaking [3,4]. A common prediction of all these extensions of the Standard Model is the appearance of new particles in the range of some hundred GeV to a few TeV.

We focus on the issue of the technicolor models of dynamical symmetry breaking which predict new particles such as Pseudo-Nambu-Goldstone-Bosons (PNGB) and vector resonances. Many of these models include colored technifermions and hence some PNGB's can be color-triplet or even color-octet particles. These color-octet scalars can be copiously produced at a hadron collider and they are the subject of this paper.

The main contribution to the color-octet PNGB masses comes from QCD. If it is assumed that technicolor dynamics scales from QCD, this contribution is in the range of 200 –

400 GeV, but their masses can be different in models with non-QCD-like dynamics [5].

Production of technicolor particles has been studied at various present and future colliders such as Tevatron [6], LEP [7], NLC [8] and the Muon Collider [9]. The impact of PNGB on rare K meson decays induced through the exchange of color-singlet π_T^\pm and color-octet π_{T8}^\pm technipions has been recently studied [11] in the context of multiscale technicolor [12] where typical limits of the order of $m_{\pi_{T8}} \geq 250$ GeV were obtained.

Of special interest is the case of the isoscalar color-octet PNGB, the so-called technieta (η_T), since it can be produced via gluon fusion through the heavy quark loop. In the near future, the upgraded 2 TeV Tevatron collider will be the most promising machine for technieta search. The channel $p\bar{p} \rightarrow \eta_T \rightarrow t\bar{t}$ was initially studied by Appelquist and Triantaphyllou [13] in the context of the one family technicolor model [14]. More recently Eichten and Lane [15] have studied the same channel in the context of walking technicolor. They concluded that a technieta with mass in the range $M_{\eta_T} = 400 - 500$ GeV doubles the top quark production cross section at Tevatron and hence it is excluded in this mass range.

In our study we would like to concentrate on the search of technieta with mass below the $t\bar{t}$ threshold, which is not constrained by the $t\bar{t}$ production process.

The $p\bar{p} \rightarrow \eta_T \rightarrow gg$ and $p\bar{p} \rightarrow \eta_T \rightarrow g\gamma$ processes were studied in the early eighties by Hayot and Napoly [16] in the framework of the one family technicolor model. They showed that, due to the signal-to-background ratio, the gluon-photon channel is preferable. Nevertheless, their results must be taken only as qualitative since no complete and detailed analysis were made.

In this letter we perform a complete realistic study of the $p\bar{p} \rightarrow \eta_T \rightarrow \gamma + \text{jet}$ process in order to understand Tevatron potentials for η_T search with the mass below the $t\bar{t}$ thresh-

old. We consider three different scenarios: the one family model [14], top-color assisted technicolor (TC2) [17] and multiscale technicolor [12].

II. EFFECTIVE COUPLINGS

The color-octet technieta couples to gluons and photons through the Adler-Bell-Jackiw anomaly [18]. This effective coupling can be written as:

$$A(\eta_T \rightarrow B_1 B_2) = \frac{S_{\eta_T B_1 B_2}}{4\pi^2 \sqrt{2} F_Q} \epsilon_{\mu\nu\alpha\beta} \epsilon_1^\mu \epsilon_2^\nu k_1^\alpha k_2^\beta \quad (1)$$

where ϵ_i^μ and k_i^μ represents the polarization and momentum of the vector boson i . In our case the factors $S_{\eta_T B_1 B_2}$ are given by [19] :

$$S_{\eta_{Ta} g_b g_c} = g_s^2 d_{abc} N_{TC} \quad (2)$$

and

$$S_{\eta_{Ta} g_b \gamma} = \frac{g_s e}{3} \delta_{ab} N_{TC} \quad (3)$$

where $g_s = \sqrt{4\pi\alpha_s}$, $e = \sqrt{4\pi\alpha}$ and α and α_s are the electromagnetic and strong coupling constant, and N_{TC} is the number of technicolors (we take $N_{TC} = 4$)

The technieta coupling to quarks can be written as:

$$A(\eta_T \rightarrow q \bar{q}) = \frac{m_q}{F_Q} \bar{u}_q \gamma_5 \frac{\lambda_a}{2} v_q. \quad (4)$$

With these couplings we can compute the technieta partial widths:

$$\Gamma(\eta_T \rightarrow gg) = \frac{5\alpha_s^2 N_{TC}^2 M_{\eta_T}^3}{384\pi^3 F_Q^2} \quad , \quad (5)$$

$$\Gamma(\eta_T \rightarrow g\gamma) \left(\frac{N_T e g_s}{4\pi F_Q} \right)^2 \frac{M_{\eta_T}^3}{576\pi} \quad (6)$$

$$\Gamma(\eta_T \rightarrow q\bar{q}) = \frac{m_q^2 M_{\eta_T} \beta_q}{16\pi F_Q^2} \quad (7)$$

where

$$\beta_q = \sqrt{1 - \frac{4m_q^2}{M_{\eta_T}^2}} \quad , \quad (8)$$

m_q is the quark mass and M_{η_T} is the technieta mass.

These expressions were used to calculate the technieta total width. From equations (5) and (6) we can see that:

$$\frac{\Gamma(\eta_T \rightarrow \gamma g)}{\Gamma(\eta_T \rightarrow gg)} = \frac{2\alpha}{15\alpha_s} = 8.7 \times 10^{-3}. \quad (9)$$

Hence, the decay channel $\eta_T \rightarrow g\gamma$ is suppressed, but due to the more manageable background it is expected to provide a larger statistical significance.

The constant F_Q that appears in the couplings is the PNGB decay constant. Its value is model-dependent. In this work we consider three values for F_Q : $F_Q = 125$ GeV for the one family technicolor model, $F_Q = 80$ GeV for top-color assisted technicolor and $F_Q = 40$ GeV for multiscale technicolor.

Some typical values of the technieta partial and total widths are shown in Table I for $\alpha_s = 0.119$ and $M_{\eta_T} = 250$ GeV.

III. SIGNAL AND BACKGROUND RATES

With the couplings discussed in the previous section we can show that the partonic cross section for the process $gg \rightarrow \eta_T \rightarrow \gamma g$ can be written as:

$$\hat{\sigma} = \frac{5\hat{s}^3\pi^3}{384} \left(\frac{N_T e g_s}{12\sqrt{2}\pi F_Q} \right)^2 \left(\frac{N_T \alpha_s}{\sqrt{2}\pi F_Q} \right)^2 \frac{1}{(\hat{s} - M_{\eta_T}^2)^2 + \Gamma_{\eta_T}^2 M_{\eta_T}^2} \quad (10)$$

We wrote a Fortran code in order to convolute the above partonic cross section with the CTEQ4M [20] partonic distribution functions (with $Q^2 = M_{\eta_T}^2$). Because the technieta coupling with quarks is proportional to the quark mass, we neglect the technieta production via $q\bar{q}\eta_T$ interaction. In the case of gluon fusion we only take into account the s -channel contribution, which is dominant at the resonance. It must be noted that gauge invariance is preserved due to the Levi-Civita tensor present in equation (3). Table II shows the cross section (in pb) calculated for different values of M_{η_T} and F_Q at $\sqrt{s} = 2000$ GeV with a cut in the transverse photon and jet momentum $p_{T\gamma,j} > 10$ GeV. These values for the cross section agree, with a precision of one percent, with a narrow width approximation. The cross section becomes sizeable for low values M_{η_T} and F_Q , being of the order of a picobarn. However, the cross section for the background $p\bar{p} \rightarrow \gamma g$ and $p\bar{p} \rightarrow \gamma q$ processes is $\sigma_{\text{back}} = 2.14 \times 10^4$ pb, which is a factor of 10^4 larger than the signal. This situation clearly shows that a detailed kinematical analysis is necessary to work out the strategy to suppress the background as strongly as possible in order to extract the signal.

IV. COMPLETE SIMULATION OF SIGNAL AND BACKGROUND

In order to perform a complete signal and background simulation we use the PYTHIA 5.7 [23] generator. Effects of jet fragmentation, initial and final state radiation (ISR+FSR) as well as smearing of the jet and the photon energies have been taken into account. Since the process $\eta_T \rightarrow \gamma g$ was absent in PYTHIA we created a generator for $gg \rightarrow \eta_T \rightarrow \gamma g$ process and linked it to PYTHIA as an external user process.

In our simulation we have used CTEQ4M structure function and have chosen $Q^2 = M_{\eta_T}^2$ for the signal.

In this framework we study, for both signal and background, distributions of the transverse photon momentum, transverse jet momentum, rapidity and invariant mass in order to find the optimal kinematical cuts for signal subtraction. These distributions are shown in Fig. 1. We can see that the ISR+FSR and energy smearing effects make the mass distribution (Fig. 1(a)) quite broad. Notice the difference in p_t distribution for photons (Fig. 1(b)) and jets (Fig. 1(c)). The fact that the distribution for jets is wider than for photons is due to initial and final state radiation.

We have found the following optimal set of kinematical cuts:

$$p_{t\gamma,\text{jet}} > \frac{M_{\eta_T}}{2} - 40 \text{ GeV} \quad (11)$$

$$M_{\eta_T} - \frac{M_{\eta_T}}{10} \leq M_{\gamma\text{jet}} \leq M_{\eta_T} + 10 \text{ GeV} \quad (12)$$

To take into account the detector pseudorapidity coverage we have chosen the following cuts for η_γ and η_{jet} :

$$|\eta_\gamma| \leq 1.5, \quad |\eta_{jet}| < 3 \quad (13)$$

Table III shows the signal and background cross sections after those cuts have been applied. It is interesting to look at the values of the significance which is written as $\frac{\mathcal{L}\sigma_{\text{signal}}}{\sqrt{\mathcal{L}\sigma_{\text{back}}}}$ and characterizes the statistical deviation of the number of the observed events from the predicted background. The significance as a function of the M_{η_T} for different technicolor models is shown in (Fig.3(a)), where we have assumed a luminosity of $\mathcal{L} = 2000 \text{ pb}^{-1}$ for the Tevatron Run II. For multiscale technicolor ($F_Q = 40 \text{ GeV}$), the significance is above the 2σ 95% CL exclusion limit for technieta mass less than 350 GeV while for a 5σ discovery criteria one obtains $M_{\eta_T} > 266 \text{ GeV}$ mass limit. For the top-color assisted technicolor model

($F_Q = 80$ GeV) one can establish only a 95% CL exclusion limit $M_{\eta_T} > 175$ GeV. For the one family technicolor model the significance is too small to establish any limits on M_{η_T} .

In our study we compared results based on PYTHIA simulation and results obtained using MADGRAPH [21] and HELAS [22] without taking into account ISR+FSR and the energy smearing effects. The corresponding significance for this case is shown in Fig.3(b). One can see that for this ideal case respective values of significance is about 2.5 times higher than in the case when we model the realistic situation using PYTHIA. The differences between Fig.3 (a) and (b) clearly shows the importance of the complete simulation of the signal and background in order to obtain realistic results.

Finally it is worth pointing out that the study of the $b\bar{b}$ signature would lead to similar bounds on the η_T mass. This is because the signal for $b\bar{b}$ final state will be roughly increased by a factor 10 (see Table I) but the background will be about two orders higher than that for $\gamma + jet$ signature. This would lead to the same values of the significance as for $\gamma + jet$ final state. However, one should take into account also the efficiency of b-tagging which will decrease the significance.

CONCLUSIONS

We have studied the potential of the upgraded Tevatron collider for the η_T search with $\eta_T \rightarrow \gamma + g$ decay signature and mass below the $t\bar{t}$ threshold. Results have been obtained for the one family model, top-color assisted technicolor and multiscale technicolor.

We found that for multiscale technicolor model, Tevatron can exclude M_{η_T} up to 350 GeV at 95%CL, while the 5σ discovery limit for η_T is 266 GeV. For the top-color assisted technicolor model one can only put a 95%CL lower limit on η_T mass equal to 175 GeV while

for one family technicolor model the significance is too small to establish any limit at all. Study of $b\bar{b}$ final state signature is not expected to give better limits on the η_T mass.

We have performed a complete simulation of the signal and background and have shown the importance of taking into account the effects of jet fragmentation, initial and final state radiation, as well as smearing of the jet and the photon energies.

ACKNOWLEDGMENTS

This work was supported by Conselho Nacional de Desenvolvimento Científico e Tecnológico (CNPq), by Fundação de Amparo à Pesquisa do Estado de São Paulo (FAPESP), and by Programa de Apoio a Núcleos de Excelência (PRONEX).

REFERENCES

- [1] Y. Golfand and E. Likhtman, *JETP Lett.* **13**, (1971)323; D. Volkov and V. Akulov, *Phys. Lett.* **B46** (1973) 109; J. Wess and B Zumino, *Nucl. Phys.* **B70** (1974) 39.
- [2] N. Arkani-Hamed, S. Dimopoulos and G. Dvali, *Phys. Lett.* **B429** (1998) 263.
- [3] S. Weinberg, *Phys. Rev.* **D19** (1979) 1277.
- [4] L. Susskind, *Phys. Rev.* **D20** (1979) 2619.
- [5] R. S. Chivukula, R. Rosenfeld, E. H. Simmons and J. Terning, in *Electroweak Symmetry Breaking and Beyond the Standard Model*, edited by T. Barklow, S. Dawson, H. E. Haber, and J. Siegrist, World Scientific.
- [6] E. Eichten and K. Lane, Proceeding of the 1996 DPF/DPB Summer Study on New Directions for High Energy Physics (Snowmass 96); K. Lane, *Phys. Lett.* **B357** (1995) 624; S. Mrenna and J. Womersley, *Phys. Lett.* **B451** (1999) 155; K. Lane, hep-ph/9903372.
- [7] V. Lubicz and P. Santorelli, *Nucl. Phys.* **B460** (1996) 3; G. Rupak and E. H. Simmons, *Phys. Lett.* **B362** (1995) 155.
- [8] W. Skiba, *Nucl. Phys.* **B470** (1996) 84; R. Rosenfeld and A. Zerwekh, *Phys. Lett.* **B418** (1998) 329.
- [9] K. Lane, talk presented at the Workshop on Physics at the First Muon Collider and at the Front End of a Muon Collider, Fermilab, November 6-9, 1997, hep-ph/98011385; E. Eichten, K. Lane and J. Womersley, *Phys. Rev. Lett.* **80** (1998) 5489.
- [10] B. Holdom, *Phys. Rev* **D24** (1981) 1441; B. Holdom, *Phys. Lett.* **B150** (1985) 301;

- K. Yamawaki, M. Bando, and K. Matumoto, *Phys. Rev. Lett.* **56** (1986) 1335; T. Appelquist, D. Karabali, and L.C.R. Wijewardhana, *Phys. Rev. Lett.* **57** (1986) 957; T. Appelquist and L.C.R. Wijewardhana, *Phys. Rev* **D35** (1987) 774; T. Appelquist and L.C.R. Wijewardhana, *Phys. Rev* **D36** (1987) 568.
- [11] Z. Xiao, L. Lü, H. Guo and G. Lu, hep-ph/9903347.
- [12] K. Lane and E. Eichten, *Phys. Lett.* **B222** (1989) 274.
- [13] T. Appelquist and G. Triantaphyllou, *Phys. Rev. Lett.* **69** (1992) 2750.
- [14] E. Farhi and L. Susskind, *Phys. Rev.* **D20** (1979) 3404.
- [15] E. Eichten and K. Lane, *Phys. Lett.* **B327** (1994) 129.
- [16] F. Hayot and O. Napoly, *Zeit. für Physik* **C7** (1981) 229.
- [17] C. T. Hill, *Phys. Lett.* **B345** (1995) 483.
- [18] S. L. Adler, *Phys. Rev.* **177** (1969) 2426; J. S. Bell and R. Jackiw, *Nuovo Cim.* **A60** (1969) 47.
- [19] J. Ellis, M. K. Gaillard, D. V. Nanopoulos and P. Sikivie, *Nucl. Phys.* **B182** (1981) 529.
- [20] H. L. Lai et al., CTEQ Collab., *Phys. Rev.* **D55** (1997) 1280.
- [21] T. Stelzer and W. F. Long, *Comput. Phys. Commun.* **81** (1994) 357.
- [22] H. Murayama, I. Watanabe and K. Hagiwara, KEK report No. 91-11, unpublished.
- [23] T. Sjöstrand, *Comput. Phys. Commun.* **82** (1994) 74.

TABLES

$\Gamma \setminus F_Q$	40 GeV	80 GeV	125 GeV
$\eta_T \rightarrow ag$	0.008	0.002	8×10^{-4}
$\eta_T \rightarrow gg$	0.929	0.232	0.095
$\eta_T \rightarrow b\bar{b}$	0.078	0.019	0.008
$\eta_T \rightarrow \text{all}$	1.015	0.254	0.104

TABLE I. Partial widths (in GeV) for $M_{\eta_T} = 250$ GeV.

$M_{\eta_T} \setminus F_Q$	40 GeV	80 GeV	125 GeV
150 GeV	6.00	1.50	0.62
200 GeV	2.58	0.65	0.27
250 GeV	1.17	0.29	0.12
300 GeV	0.55	0.14	0.06
340 GeV	0.31	0.08	0.03

TABLE II. Total cross section in pb for the process $p\bar{p} \rightarrow \eta_T \rightarrow g\gamma$ with $\sqrt{s} = 2000$ GeV.

$M_{\eta_T} \setminus F_Q$	40 GeV	80 GeV	125 GeV	Background
150 GeV	1.53	0.38	0.16	60.72
200 GeV	0.63	0.16	0.06	15.51
250 GeV	0.26	0.07	0.03	4.53
300 GeV	0.11	0.03	0.01	1.72
340 GeV	0.06	0.01	6×10^{-3}	0.94

TABLE III. Signal and background cross sections in pb for $\sqrt{s} = 2000$ GeV after cuts.

FIGURES

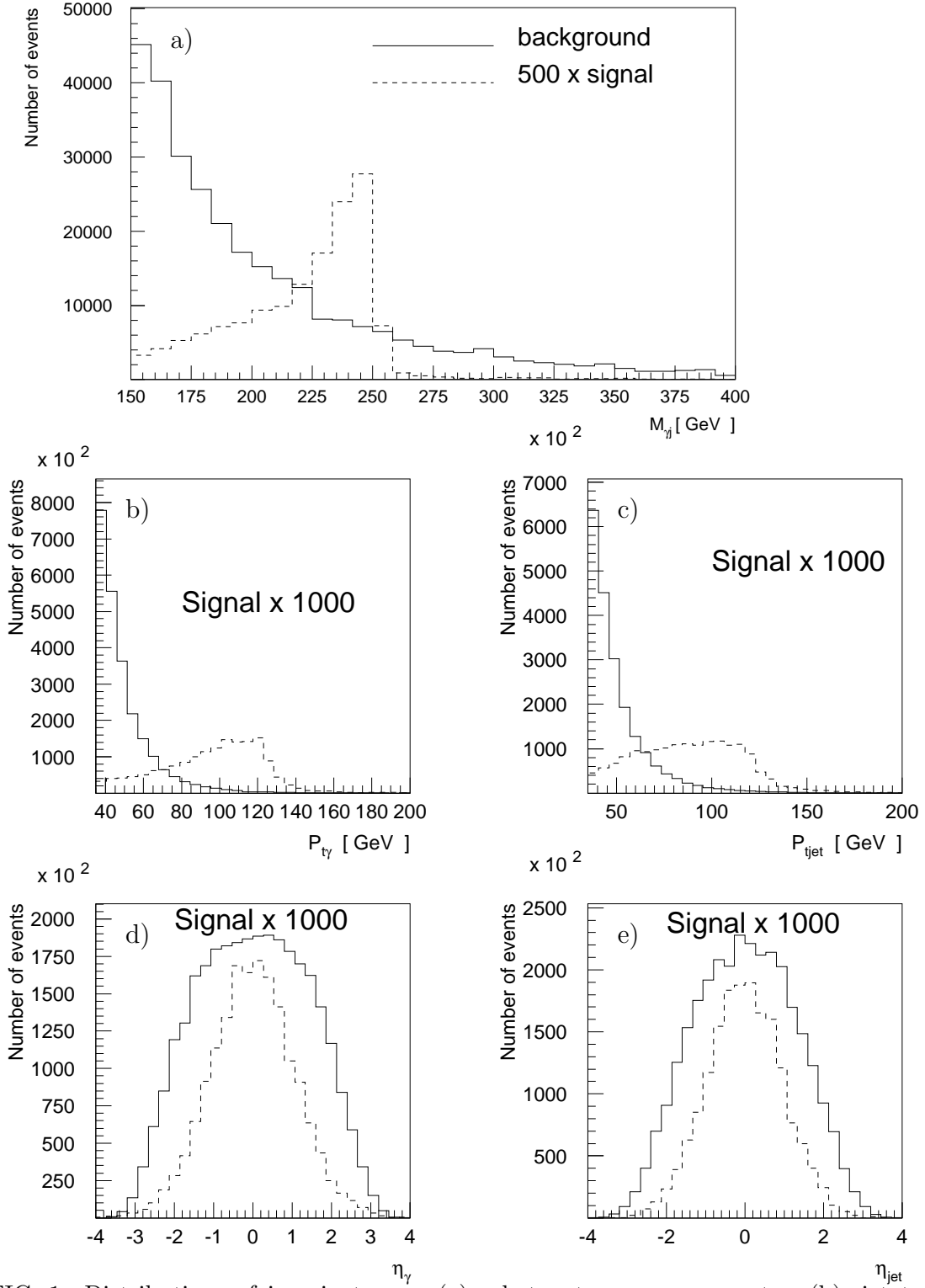


FIG. 1. Distributions of invariant mass (a), photon transverse momentum (b), jet transverse momentum (c), photon rapidity (d) and jet rapidity (e) for signal (dashed line) and background (solid line) before any cut. We have assumed $M_{\eta_T} = 250$ GeV and $F_Q = 40$ GeV.

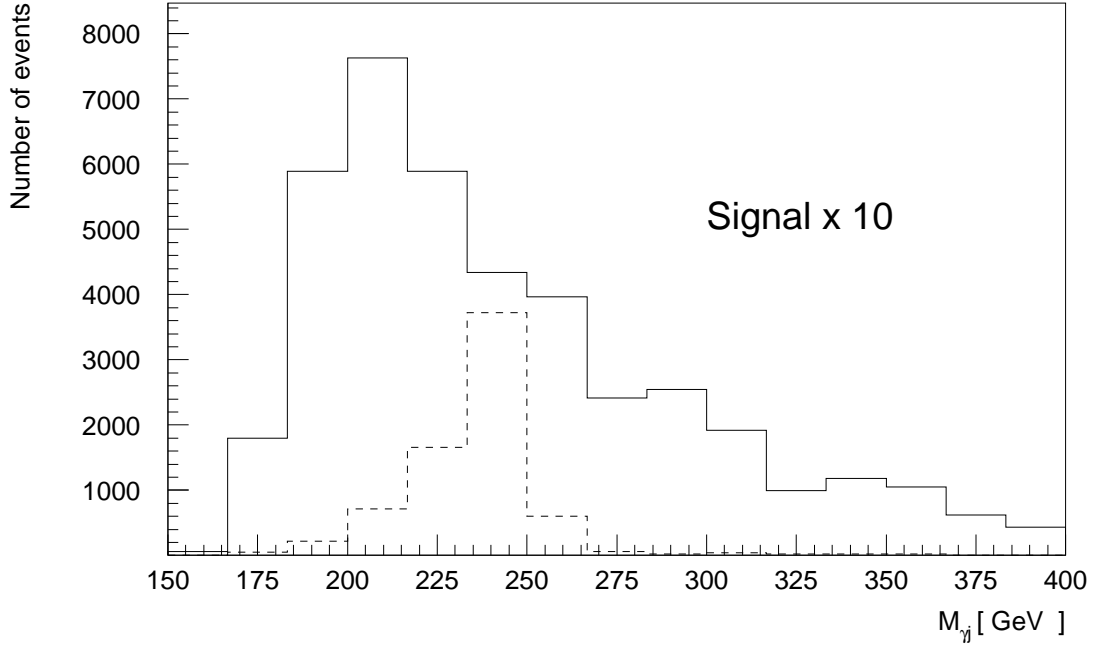


FIG. 2. Invariant mass distribution for signal (dashed line) and background (solid line) after cuts, $M_{\eta_T} = 250$ GeV and $F_Q = 40$ GeV.

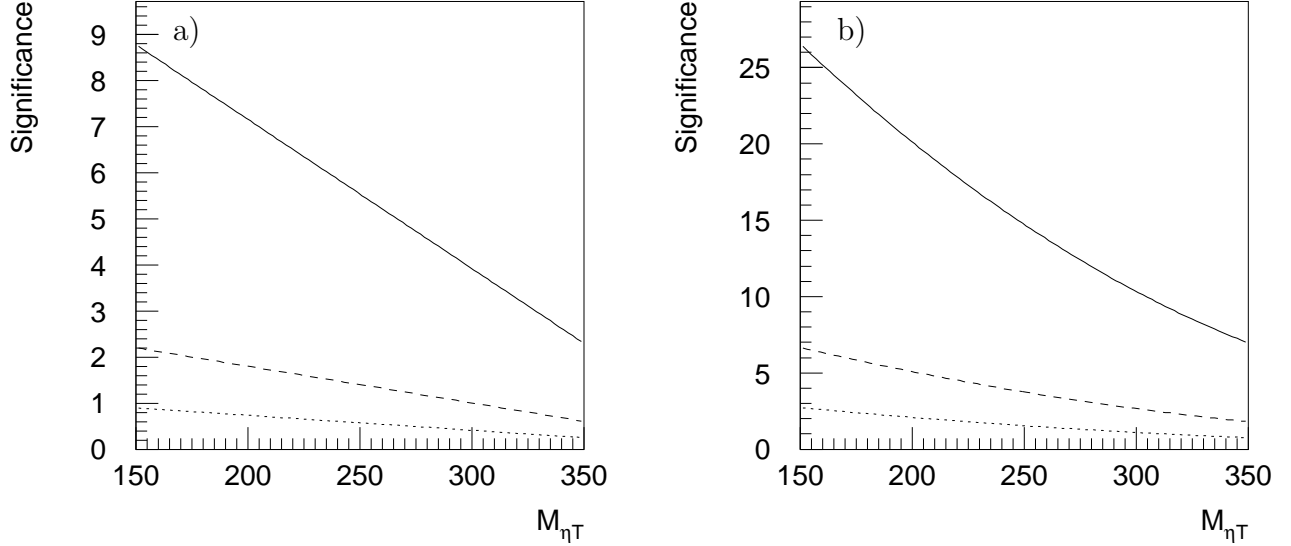


FIG. 3. Significance as a function of M_{η_T} for multiscale technicolor (solid line), top-color assisted technicolor (dashed line) and one family technicolor (dotted line), based on results obtained with (a) and without (b) taking into account ISR+FSR and energy smearing effects.